BMC Neurology

RESEARCH

Open Access

Dysregulated interleukin networks drive immune heterogeneity in Alzheimer's disease: an immunogenomic approach to subgroup classification and predictive modeling

Bin Zhang[1], Binglei Xu[1], Ruoxian Zhang[2], Baoying Gong[1] and Jianwen Guo[3*]

Abstract

Background Alzheimer's Disease (AD) is marked by intricate immunological alterations, including the dysregulation of interleukin signaling. This study investigates the differential expression and potential roles of interleukins and their receptors in AD patients.

Methods We analyzed the GSE48350 dataset to assess the single-sample Gene Set Enrichment Analysis (ssGSEA) scores for interleukins and their receptors between normal and AD groups. Differentially expressed interleukin-related genes (DIGs) were identified. Enrichment analysis was conducted to understand functional implications. LASSO and logistic regression were used to identify key interleukin genes, which were employed to construct a predictive nomogram. This model was validated using the GSE132903 dataset. Unsupervised clustering and immune cell infiltration analyses were performed to examine AD patient heterogeneity.

Results The ssGSEA scores indicated significantly elevated interleukin and receptor levels in AD patients. A total of 23 DIGs were discovered, and the enrichment analysis emphasized their participation in immune signaling pathways. The nomogram based on key interleukin genes demonstrated strong predictive capability, with an AUC of 0.882 in the training set and 0.837 in the validation set. Unsupervised clustering revealed two AD subgroups with distinct immune profiles and pathway activities. Subgroup C2 exhibited higher immune cell infiltration and pathway activity than subgroup C1.

Conclusion Interleukins and their receptors are significantly upregulated in AD patients, with distinct immune profiles identified in AD subgroups. The predictive nomogram effectively stratifies AD patients based on interleukin gene expression. These findings provide insights into AD's immunological landscape and suggest potential biomarkers for personalized therapeutic strategies.

Keywords Alzheimer's disease, Interleukins, Immune profiling, Predictive nomogram, Immune subtypes

*Correspondence:
Jianwen Guo
guojw_n@163.com
[1]Guangzhou University of Chinese Medicine, Guangzhou, Guangdong Province 510405, China
[2]Institutes of Biomedical Sciences, Shanghai Medical College, Fudan University, Shanghai 200032, China
[3]The Second Affiliated Hospital of Guangzhou, Guangdong Provincial Hospital of Traditional Chinese Medicine, University of Chinese Medicine, N. 111 Dade Road, Yuexiu District, Guangzhou City 510030, Guangdong Province, China

Introduction

Alzheimer's Disease (AD) is a progressive neurodegenerative disorder characterized by cognitive decline, memory loss, and functional impairment. It affects millions of individuals worldwide, posing significant challenges to healthcare systems and caregivers [1, 2]. Emerging evidence suggests AD is not a single disease entity but rather comprises distinct subtypes with heterogeneous pathological features and progression patterns. Current classifications identify subtypes based on: (1) regional atrophy patterns (hippocampal-sparing, typical, and limbic-predominant), (2) cerebrospinal fluid biomarker profiles, and (3) inflammatory signatures (inflammatory, non-inflammatory, and cortical subtypes) [3–5]. Notably, the inflammatory subtype demonstrates heightened activation of microglia and astroglia, increased cytokine production, and more rapid cognitive decline compared to other subtypes [6, 7]. Despite extensive research, the exact pathogenesis of AD remains elusive, with multiple hypotheses proposed, including amyloid-beta (Aβ) plaque deposition, tau protein hyperphosphorylation, oxidative stress, and neuroinflammation [8, 9]. Recent studies have highlighted the pivotal role of neuroinflammation in AD, implicating microglial activation and the release of pro-inflammatory cytokines in neuronal damage. This chronic inflammation exacerbates synaptic dysfunction and accelerates disease progression [10, 11]. Identifying AD subtypes has profound therapeutic implications, as different subgroups may respond preferentially to anti-amyloid therapies, tau-targeted interventions, or immunomodulatory approaches [12, 13]. However, current subtyping frameworks lack integration of interleukin network dynamics and immunogenomic signatures - a gap this study aims to address through comprehensive profiling of interleukin-related pathways.

The pathological role of interleukins in AD is multifaceted, encompassing several mechanisms that contribute to neurodegeneration. Dysregulated interleukin signaling can lead to chronic inflammation within the central nervous system (CNS), a hallmark of AD [14]. This chronic inflammation is primarily driven by the overproduction of pro-inflammatory interleukins, such as IL-1β, IL-6, and IL-18, which are known to exacerbate neuronal damage and promote the formation of amyloid plaques and neurofibrillary tangles [15]. Administration of IL-33 leads to a decrease in soluble β-amyloid concentrations and the accumulation of amyloid plaques is curbed through the enhancement of microglial recruitment and their ability to ingest β-amyloid [16]. Additionally, IL-6 has been implicated in the phosphorylation of tau protein, a critical event in the formation of neurofibrillary tangles [17]. The persistent activation of these interleukin-mediated pathways not only contributes to the pathological features of AD but also disrupts neuronal communication and synaptic function, leading to cognitive decline. Moreover, recent genetic studies have underscored the importance of interleukin-related genes in AD. Polymorphisms in genes encoding interleukins and their receptors have been associated with an increased risk of developing AD. For instance, variants in the IL-10, IL-6, and IL-1β genes have been linked to altered expression levels and activity, influencing the individual's susceptibility to neuroinflammation and AD progression [15, 18, 19, 20]. These genetic associations highlight the potential of interleukin signaling pathways as therapeutic targets.

This study aims to investigate the differential expression of interleukins and their receptors in AD patients compared to normal individuals. By leveraging the GSE48350 dataset, we conducted a single-sample Gene Set Enrichment Analysis (ssGSEA) to quantify the expression levels of interleukin-related genes. Furthermore, we identified differentially expressed interleukin-related genes (DIGs) and explored their functional implications through enrichment analysis. To pinpoint key interleukin genes with potential diagnostic value, we employed LASSO and logistic regression models. These key genes were subsequently used to construct a predictive nomogram, which was validated using the GSE132903 dataset. In addition, we performed unsupervised clustering and immune cell infiltration analyses to examine the heterogeneity among AD patients. Our findings revealed distinct immune profiles and pathway activities between the identified subgroups, highlighting the complexity of AD's immunological landscape.

The study's significance lies in its potential to uncover novel biomarkers for AD diagnosis and to provide insights into personalized therapeutic strategies targeting interleukin dysregulation. By elucidating the roles of interleukins in AD, we aim to contribute to a deeper understanding of the disease and to facilitate the development of targeted interventions that can mitigate its progression.

Methods

Data acquisition and data preprocessing

The dataset utilized for our investigation was obtained from the GEO repository (https://www.ncbi.nlm.nih.gov/geo/). Our analysis encompassed two cohorts: GSE48350, comprising 173 samples from the normal control group and 80 samples from the AD group, and GSE132903, which included 98 normal control and 97 AD patient samples. GSE48350 served as the exploratory dataset, while GSE132903 was employed as the validation dataset. Tables S1 and Table S2 present the demographic characteristics of these two datasets. Before conducting data analysis, the unprocessed matrix files were extracted and standardized with the assistance of the Affy software package.

Evaluation of the interleukin pathways score in AD

Two gene sets linked to interleukin-related pathways (interleukins and interleukin receptors) were retrieved from the ImmPort database (http://www.immport.org). The ssGSEA algorithm was utilized to compute the interleukin-related pathway scores for individual samples, which were presented through box plots. In total, 89 interleukin pathways-related genes (IGs) were identified within these gene sets.

Identification and analysis of differentially regulated interleukin-associated genes (DIGs)

Based on the gene expression profiles of the 89 interleukin genes (IGs), the identification of DIGs was performed by comparing the normal and AD groups using the limma package (version 3.22.7). Criteria for selection were set at an adjusted p-value lower than 0.05 and a|log-fold change (FC)| greater than 1. The network of protein-protein interactions (PPI) in the DIGs was constructed by leveraging the STRING database (https://cn.string-db.org/), with a confidence score threshold of 0.7 set as the criterion. The visualization of the network was accomplished using the Cytoscape software tool. We utilized clusterProfiler and enrichplot packages for conducting KEGG enrichment analysis and GO functional annotation. A significance threshold was defined, wherein any adjusted p-value below 0.05 was deemed significant.

LASSO and logistic regression were employed for the identification of feature genes

In our study, we utilized LASSO regression analysis to pinpoint key genes associated with AD by analyzing the expression patterns of DIGs. The glmnet (version 4.1.7) software package was employed to carry out the LASSO regression using the glmnet() function and 10-fold cross-validation performed via the cv.glmnet() function to determine the optimal penalty parameter. Following this, logistic regression analysis was conducted using the lrm() function from the rms package (version 6.4.0) to further identify crucial DIGs, with default parameters retained except for specifying maximum iterations = 200.

Development and validation of a nomogram

In the development of the nomogram, we leveraged the lrm() function from the rms package (version 6.4.0) to integrate the signature genes identified through logistic regression. Specifically, the nomogram() function was employed to construct the nomogram, using the results from the logistic regression model as input. The lrm() function used these signature genes as predictors, with the outcome being AD diagnosis. For the nomogram construction, we included the 8 key signature genes identified by logistic regression: IL1R2, IFNLR1, IL10RA, IL4R, IL1RL2, IL22RA1, IL5, and IL12A. The weights associated with each gene in the nomogram correspond to their respective regression coefficients from the logistic model, which reflect the contribution of each gene to the total risk prediction. These coefficients were converted to points, and the final nomogram was constructed by summing the points for each gene to predict the probability of AD. The diagnostic performance of the nomogram was evaluated by constructing a Receiver Operating Characteristic (ROC) curve using the roc() function from the pROC package (version 1.18.0). The area under the curve (AUC) was calculated to assess the model's discriminatory power. Furthermore, the model's precision was validated using calibration plots and decision curve analysis (DCA), both of which were performed using functions from the rms package. The nomogram developed in the training cohort (GSE48350) was externally validated using the GSE132903 dataset without recalibration or re-estimation of coefficients.

Identification of disease subtypes related to interleukins in AD

To elucidate the correlation between interleukins and AD, we utilized the ConsensusClusterPlus package to perform clustering analysis on the expression profiles of DIGs. The optimal cluster count, represented by the "k" value, was determined from the cumulative distribution function plot. Additionally, we executed differential expression analysis across distinct disease subgroups using the limma package and conducted Gene Set Enrichment Analysis (GSEA) between these subgroups employing the GSEA software.

Examination of the immunological microenvironment

To quantify the abundance of 24 distinct immune cell subsets and the activation states of 16 immune response pathways, single-sample gene set enrichment analysis (ssGSEA) was applied. The gene sets delineating immune cell subsets were curated from existing studies [21], whereas those pertaining to immune response pathways were obtained from the ImmPort repository (http://www.immport.org) (**Table S3**). These gene sets served to determine the enrichment levels of various immune components. A Pearson correlation analysis was performed to investigate the connection between the signature genes and the quantities of immune cell elements. Relationships with p-values less than 0.05 were deemed to be statistically significant, suggesting a clear link between the signature genes and immune characteristics.

Results

Enrichment analysis and differential expression of interleukin levels in Alzheimer's Disease patients

Figure 1A depicts the ssGSEA scores for interleukins and interleukin receptor pathways between normal and AD

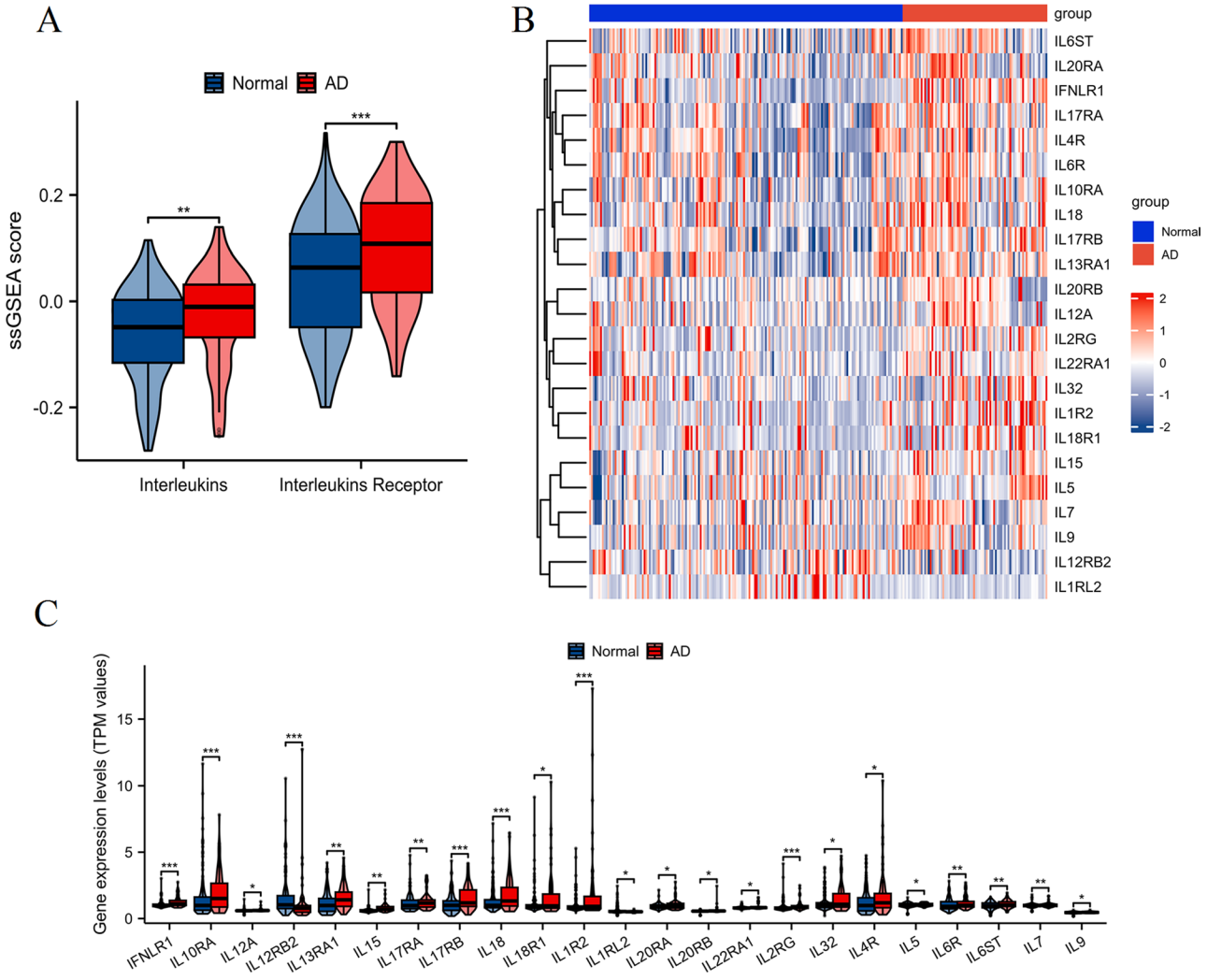

Fig. 1 Differential expression of interleukins and interleukin receptors in normal and AD. (**A**) Violin plots showing ssGSEA scores for interleukins and interleukin receptors in normal (blue) and AD (red) groups. (**B**) Heatmap illustrating the hierarchical clustering of gene expression levels for DIGs in normal (blue) and AD (red) groups. The expression values for each gene were standardized to z-scores to facilitate comparison across samples. (**C**) Violin plots of gene expression levels (TPM values) for DIGs in normal (blue) and AD (red) group. *$p < 0.05$, **$p < 0.01$, ***$p < 0.001$

groups in the GSE48350 dataset. The AD group shows a significant increase in the ssGSEA scores for both interleukins ($p < 0.01$) and their receptors ($p < 0.001$) compared to the normal control group. This suggests an overall elevation in the expression levels of interleukins and their receptors in AD patients. Figure 1B presents the heatmap of 23 DIGs between the normal and AD groups. The hierarchical clustering shows distinctive expression patterns, with the AD group exhibiting higher expression levels (represented in red) of several interleukin-related genes compared to the normal group (represented in blue). Figure 1C provides a detailed comparison of individual interleukin-related gene expressions between normal and AD groups using violin plots. The plots highlight several genes with significant differential expression. For example, the expression of IL1R2, IL17RB, IFNLR1, IL10RA, IL18, and IL2RG is significantly different in the AD group compared to the normal group ($p < 0.001$). Similarly, IL6R, IL13RA1, IL6ST, IL17RA, IL15, and IL7 also show significant differences in expression ($p < 0.01$). Furthermore, IL20RB, IL18R1, IL22RA1, IL4R, IL20RA, IL32, IL5, IL12A, and IL9 display differential expression ($p < 0.05$). On the other hand, IL12RB2 and IL1RL2 exhibit significant decreases in expression in the AD group ($p < 0.001$ and $p < 0.005$, respectively). These results demonstrate that multiple interleukins and their receptors are upregulated in AD patients, indicating their potential role in the pathophysiology of AD.

Protein-protein interaction (PPI) network and enrichment analysis of differentially expressed interleukin-related genes in AD

Figure 2A shows the PPI network constructed for the interleukin-related genes that were differentially

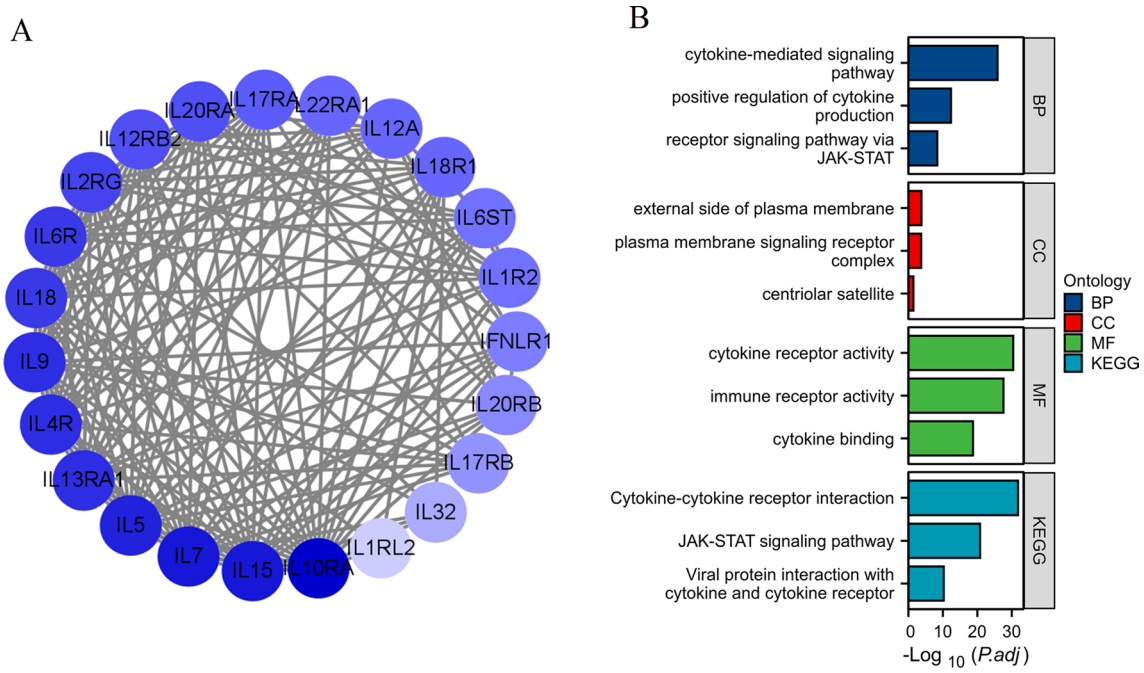

Fig. 2 PPI network and functional enrichment analysis of differentially expressed interleukin genes in AD. (**A**) PPI network: Nodes represent differentially expressed interleukin genes between normal and AD groups, while edges represent predicted protein-protein interactions. (**B**) Enrichment analysis: Bar plots display significantly enriched terms for the differentially expressed interleukin genes across four categories (BP, CC, MF, and KEGG)

expressed between normal and AD groups. Nodes represent the interleukin genes, and edges signify the predicted interactions between these proteins. Extensive interconnections can be observed in the network, indicating a complex interaction landscape and suggesting potential coordinated roles of these genes in AD pathophysiology. The results of Fig. 2B show that the differentially expressed interleukin-related genes were enriched in various ontology and pathway terms. In the Biological Process (BP) category, terms such as cytokine-mediated signaling pathway, positive regulation of cytokine production, and receptor signaling pathway via JAK-STAT were significantly enriched. The Cellular Component (CC) category included terms like the external side of plasma membrane, plasma membrane signaling receptor complex, and centriolar satellite. Molecular Function (MF) terms that were enriched included cytokine receptor activity, immune receptor activity, and cytokine binding. The KEGG Pathways analysis revealed enrichment in pathways such as cytokine-cytokine receptor interaction, JAK-STAT signaling pathway, and viral protein interaction with cytokine and cytokine receptors. The enrichment analysis highlights that the differentially expressed interleukin genes are primarily involved in immune signaling pathways, especially the JAK-STAT pathway and cytokine-mediated signaling, which are known to play crucial roles in inflammatory responses. The specific enrichment in the plasma membrane-related categories suggests that many of these proteins are membrane-associated, which aligns with their roles as receptors and signaling molecules.

Identification of key interleukin genes in AD and nomogram construction using LASSO and Logistic regression

Figure 3A displays the LASSO regression result for identifying key interleukin genes. In this analysis, several interleukin genes (IL1R2, IL17RB, IL12RB2, IFNLR1, IL10RA, IL6ST, IL4R, IL32, IL6R, IL1RL2, IL22RA1, IL20RB, IL5 and IL12A) were identified as key variables based on their minimal cross-validated error. Subsequently, we conducted a logistic regression analysis incorporating these 14 genes, identifying 8 pivotal genes (IL1R2, IFNLR1, IL10RA, IL4R, IL1RL2, IL22RA1, IL5, and IL12A) that demonstrated statistically significant (p-values < 0.05). This indicates their potential role as biomarkers for AD patients (Table 1). Figure 3B illustrates the nomogram constructed using the training dataset (GSE48350) based on the 8 key interleukin genes identified through logistic regression. This nomogram serves as the foundational model for predicting AD risk. Each variable's contribution to the total points is depicted, facilitating individualized risk assessment based on gene expression. Figure 3C shows the ROC curve of the training cohort (GSE48350), yielding an AUC of 0.882, reflecting the model's discriminative performance in the development phase. Figure 3D presents the calibration plot, demonstrating the agreement between the

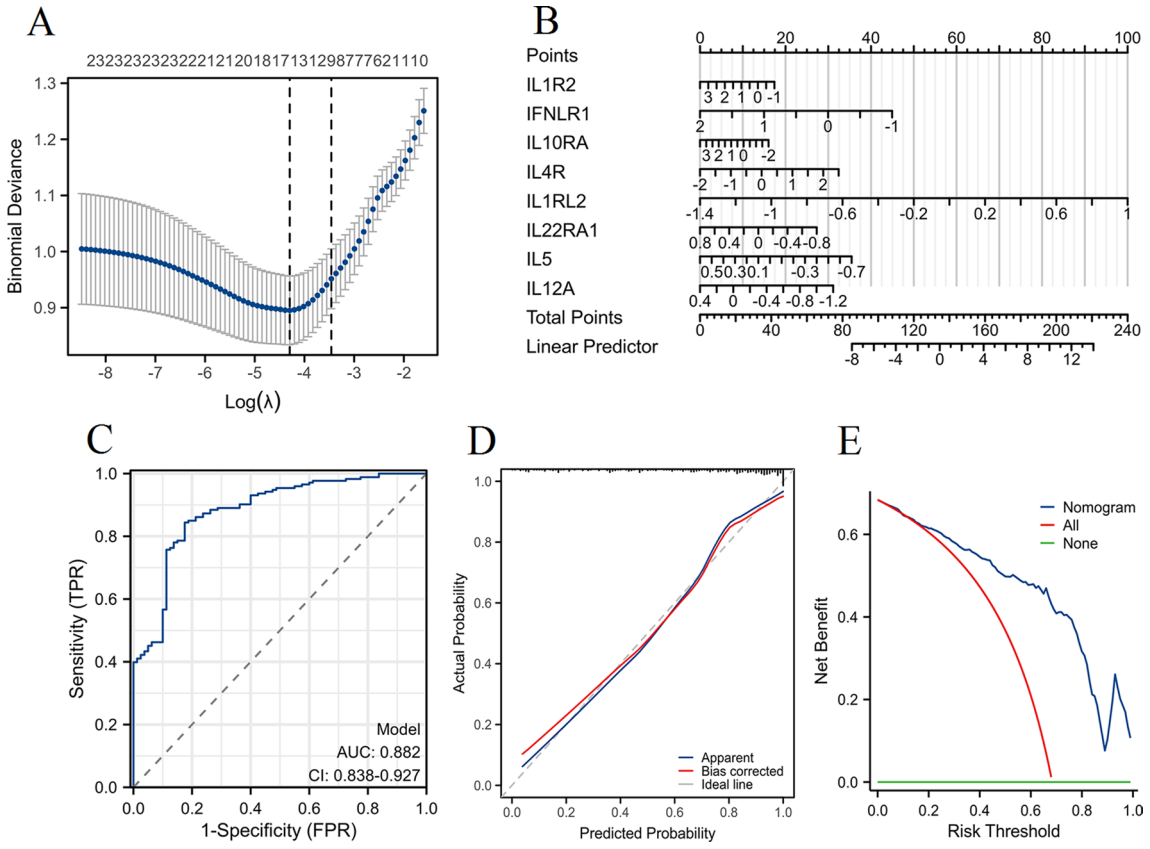

Fig. 3 Identification of key interleukin genes in AD and construction of a predictive nomogram. (**A**) The plot of binomial deviance versus log(λ) shows the process of selecting key interleukin genes based on the minimum cross-validated error, identifying the most relevant genes for AD prediction. (**B**) The nomogram illustrates how the selected key interleukin genes (IL1R2, IFNLR1, IL10RA, IL4R, IL1RL2, IL22RA1, IL5, and IL12A) contribute to the total score, which predicts the probability of AD. (**C**) The ROC curve displays the performance of the logistic regression model based on the selected genes. (**D**) The calibration curve shows the agreement between predicted probabilities from the nomogram and actual observed outcomes. (**E**) The DCA compares the net benefit of using the nomogram for clinical decision-making across a range of risk thresholds

Table 1 The results of logistic regression analysis

Characteristics	Total(*N*)	Univariate analysis		Multivariate analysis	
		Odds Ratio (95% CI)	*P* value	Odds Ratio (95% CI)	*P* value
IL1R2	253	0.455 (0.325–0.636)	**< 0.001**	0.560 (0.328–0.957)	**0.034**
IL17RB	253	0.523 (0.382–0.716)	**< 0.001**	0.761 (0.446–1.296)	0.315
IL12RB2	253	1.873 (1.360–2.580)	**< 0.001**	1.206 (0.780–1.863)	0.400
IFNLR1	253	0.150 (0.082–0.274)	**< 0.001**	0.074 (0.029–0.192)	**< 0.001**
IL10RA	253	0.601 (0.453–0.797)	**< 0.001**	0.563 (0.337–0.940)	**0.028**
IL6ST	253	0.588 (0.417–0.829)	**0.002**	0.726 (0.433–1.219)	0.226
IL4R	253	0.687 (0.513–0.920)	**0.012**	3.494 (1.661–7.351)	**< 0.001**
IL32	253	0.511 (0.326–0.800)	**0.003**	0.667 (0.329–1.354)	0.262
IL6R	253	0.511 (0.308–0.847)	**0.009**	2.611 (0.822–8.296)	0.104
IL1RL2	253	27.242 (3.914–189.614)	**< 0.001**	952.583 (25.751–35237.6698)	**< 0.001**
IL22RA1	253	0.039 (0.007–0.215)	**< 0.001**	0.079 (0.010–0.631)	**0.017**
IL20RB	253	0.074 (0.013–0.414)	**0.003**	0.092 (0.005–1.543)	0.097
IL5	253	0.140 (0.033–0.599)	**0.008**	0.023 (0.002–0.277)	**0.003**
IL12A	253	0.161 (0.037–0.699)	**0.015**	0.074 (0.007–0.805)	**0.032**

predicted probabilities from the nomogram and the actual observed probabilities. The bias-corrected line (red) closely aligns with the ideal line (gray), indicating that the model's predictions are well-calibrated and reliable. Figure 3E depicts the decision curve analysis (DCA) for the constructed nomogram. The DCA compares the net benefits of the nomogram, considering different risk thresholds. The blue line (nomogram) shows a higher net benefit compared to the "All" and "None" strategies, indicating that the nomogram provides a meaningful improvement in decision-making regarding AD risk.

Validation of the established nomogram using the GSE132903 dataset

Figure 4A demonstrates the external validation of the nomogram (originally developed in Fig. 3B) by applying it to the independent GSE132903 dataset. The model retained the same gene coefficients and scoring system without re-training. Figure 4B illustrates the ROC curve of the validation cohort (GSE132903), achieving an AUC of 0.837, confirming the generalizability of the nomogram. Figure 4C presents the calibration plot for the nomogram in the validation cohort, showing the relationship between predicted probabilities and actual observed outcomes. The bias-corrected line (red) closely follows the ideal line (gray), indicating that the predictions made by the nomogram are well-calibrated and accurate. Figure 4D depicts the DCA for the nomogram, comparing the net benefits across different risk thresholds. The blue line (nomogram) has a higher net benefit compared to the "All" and "None" strategies, validating the clinical utility of the nomogram for decision-making regarding AD risk in the independent validation dataset. Overall, the validation results confirm that the established nomogram provides robust and accurate predictions of AD in an independent cohort.

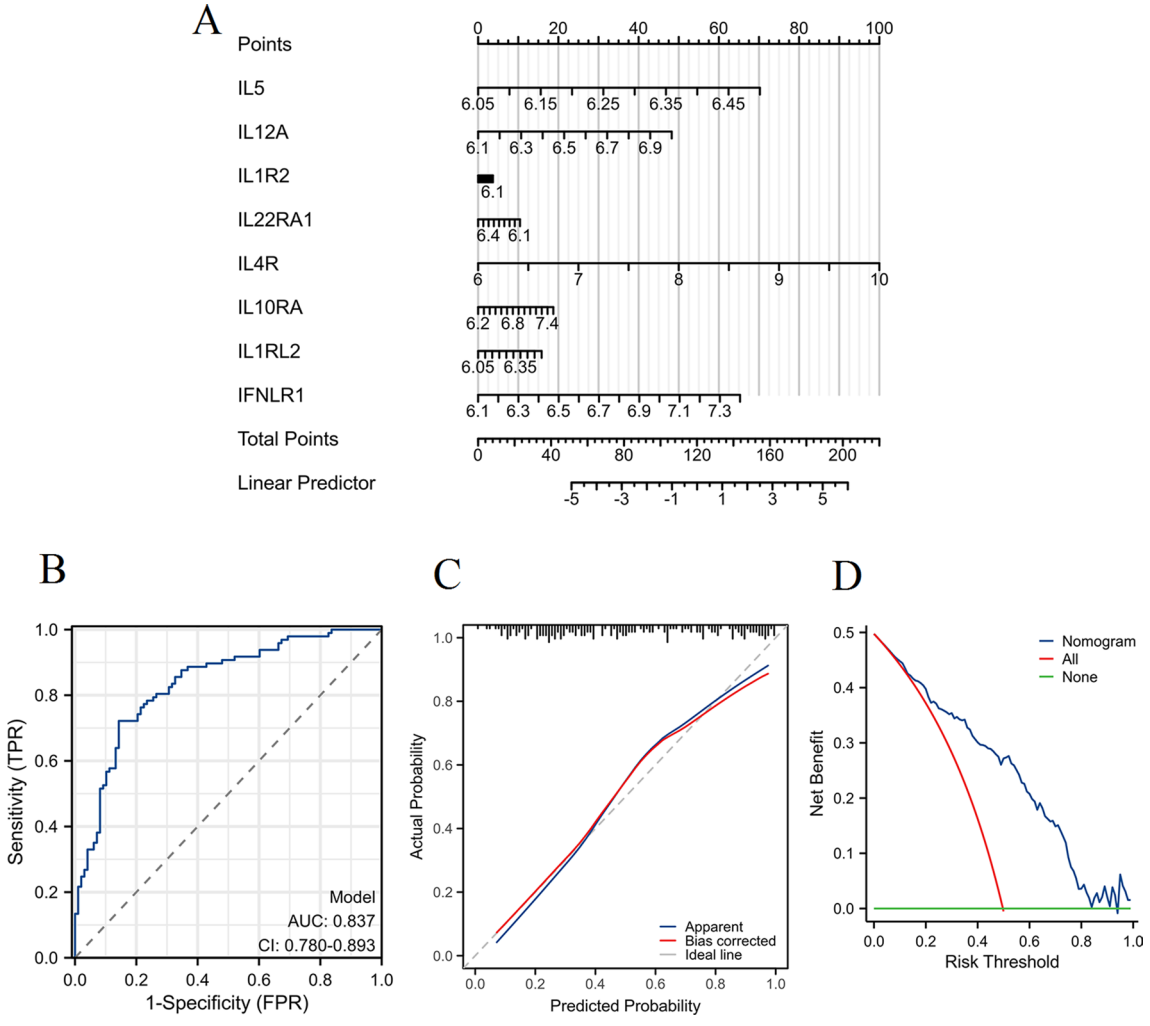

Fig. 4 Validation of the predictive nomogram for AD using the GSE132903 dataset. (**A**) A nomogram was constructed based on the GSE132903 dataset incorporating key interleukin genes. (**B**) ROC curve for the validation cohort. (**C**) Calibration plot. (**D**) The DCA plot compares the net benefit of using the nomogram for clinical decision-making

Unsupervised clustering analysis of AD patients based on interleukin-related differentially expressed genes

Figure 5A illustrates the consensus clustering heatmap for AD patients based on interleukin-related differentially expressed genes. The heatmap reveals two distinct clusters (C1 and C2) characterized by differing expression patterns of these genes. Figure 5B presents the relative change in the area under the cumulative distribution function (CDF) curve, plotted to determine the optimal number of clusters (K). The curve exhibits a peak at K = 2 (highest relative change), followed by a gradual decline. While the absolute reduction in slope diminishes at

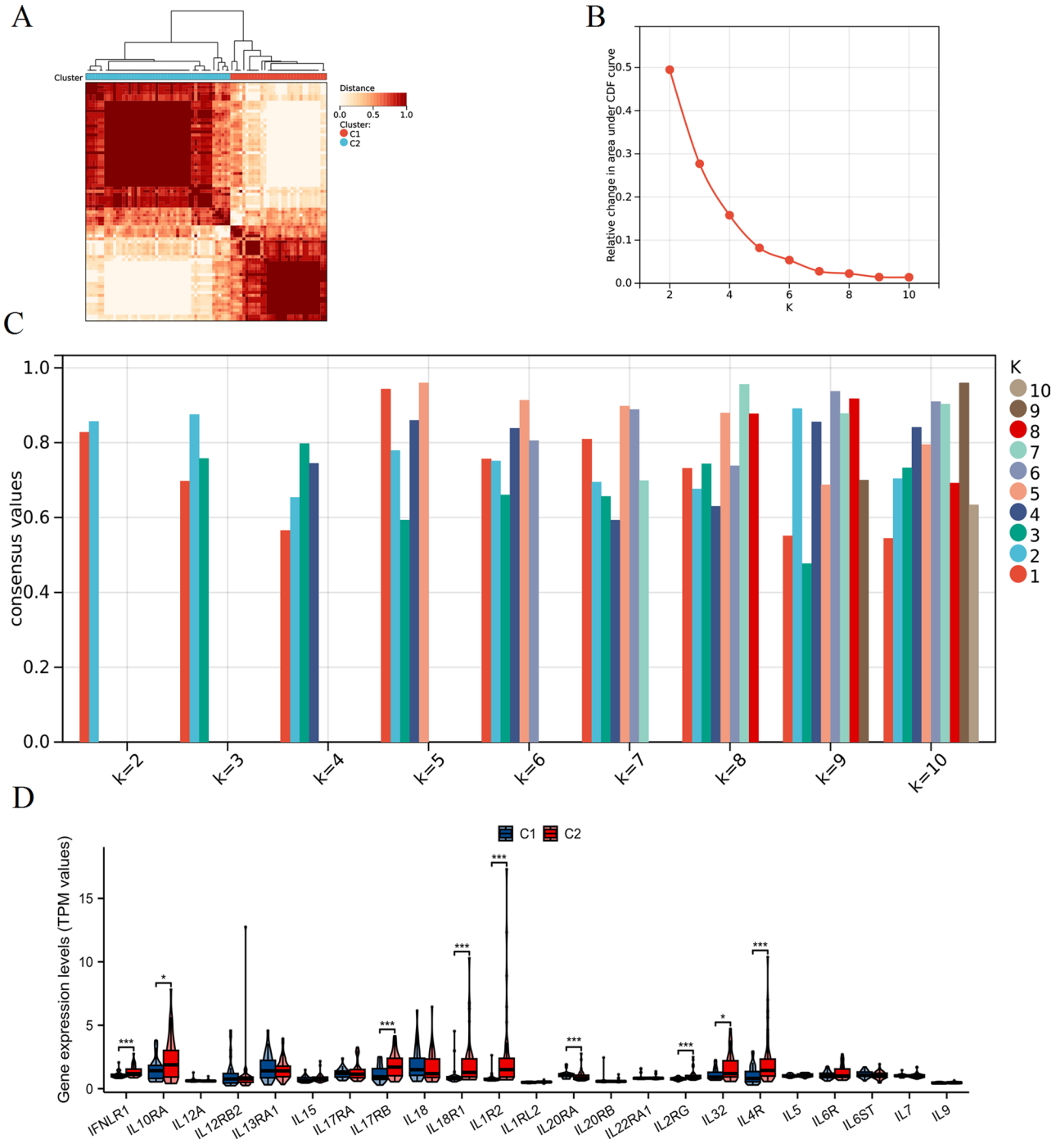

Fig. 5 Unsupervised clustering of AD patients. (**A**) Consensus clustering heatmap. (**B**) Relative change in area under CDF curve. (**C**) Consensus values for different cluster numbers. (**D**) Violin plots comparing the expression levels of (TPM values) interleukin-related genes between clusters C1 (blue) and C2 (red)

larger K values, the elbow criterion prioritizes the most pronounced inflection point, which corresponds to K = 2. Figure 5C shows the consensus values for varying cluster numbers (K = 2 to K = 10). The consensus values for K = 2 exhibit the highest stability and robustness, supporting the decision to select two clusters. Figure 5D compares the gene expression levels of interleukin-related genes between the two identified clusters (C1 and C2) using violin plots. The expression levels of several genes show significant differences between the clusters: IL1R2, IL17RB, IFNLR1, IL10RA, IL4R, IL18R1, IL32, and ILRG are significantly upregulated in cluster C2 compared to cluster C1 ($p < 0.001$, $p < 0.01$, $p < 0.05$). In contrast, IL20RA is significantly downregulated in cluster C2 compared to cluster C1 ($p < 0.001$). These results indicate that AD patients can be successfully stratified into two subgroups based on the expression patterns of interleukin-related genes. The significant differences in gene expression profiles between clusters C1 and C2 suggest potential biological heterogeneity among AD patients. Understanding these differences may provide insights into distinct pathological mechanisms and could guide personalized therapeutic approaches for AD.

Immune cell infiltration and immune-related pathway activity in AD subgroups.

Figure 6A shows the ssGSEA scores comparing immune cell infiltration between normal and AD groups. The AD group exhibits significantly higher infiltration levels of several immune cell types, including aDC, CD8 T cells, DC, Macrophages, Neutrophils, NK cells, T helper cells, Tcm, Tem, Tgd, Th 17 cells, and Treg ($p < 0.05$, $p < 0.01$, $p < 0.001$). These findings suggest an enhanced immune response in the AD group compared to normal controls. Figure 6B further analyzes the immune cell infiltration between the two interleukin-related AD subgroups (C1 and C2) identified through unsupervised clustering. Significant differences in immune cell infiltration are observed: Subgroup C2 shows higher levels of aDC, CD8 T cells, Cytotoxic cells, Neutrophils, Tem, and Treg compared to subgroup C1 ($p < 0.05$, $p < 0.01$, $p < 0.001$). Figure 6C presents a correlation heatmap showing the relationship between key interleukin genes and immune cell types, with correlation coefficients (|Cor|) depicted. The most significant correlations ($|Cor| > 0.5$, $p < 0.001$) involve genes such as IL10RA, IL4R, and IL5 with various immune cells, underscoring specific gene-cell interactions that may underpin the immune heterogeneity observed in AD. Figure 6D illustrates ssGSEA scores comparing the activity of immune-related pathways between the two AD subgroups (C1 and C2). Several pathways show significant differences in activity: cytokine receptors, interleukins receptors, natural killer cell cytotoxicity, TCR signaling pathways, TGFb family member, TGFb family member receptor, and TNF family members receptors pathways exhibit significantly higher activity in subgroup C2 ($p < 0.05$, $p < 0.01$, $p < 0.001$). This indicates that subgroup C2 is characterized by heightened immune pathway activity, which may contribute to more pronounced immune responses and inflammation compared to subgroup C1. These analyses emphasize the differential immune landscapes between AD patients and normal controls, as well as among AD subgroups characterized by distinct interleukin gene expression patterns. The observed variations in immune cell infiltration and pathway activities provide insights into the underlying immunological heterogeneity of AD, which could inform tailored therapeutic strategies targeting specific immune pathways for different patient subgroups.

Differential expression and GSEA of interleukin-related AD subgroups

Figure 7A shows a volcano plot illustrating the differentially expressed genes (DEGs) between the two interleukin-related AD subgroups (C1 and C2). Red points indicate significantly upregulated genes in cluster C2 (1,040 genes), while blue points denote significantly downregulated genes in cluster C2 (749 genes) (Table S4). Figure 7B presents a heatmap of the top 50 DEGs between the two AD subgroups, with hierarchical clustering. The heatmap shows a clear separation between clusters C1 and C2, with genes upregulated in cluster C2 (red) and downregulated in cluster C2 (blue). This distinct clustering of gene expression profiles further corroborates the differences between the two subgroups, suggesting underlying molecular heterogeneity. Figure 7C depicts the results of GSEA, comparing enriched pathways between subgroups C1 and C2. The top enriched pathways in cluster C1 include: Tryptophan Metabolism (ES = 0.3150, $p = 0.0121$), Alanine, Aspartate, and Glutamate Metabolism (ES = 0.6179, $p = 0.0130$), Porphyrin and Chlorophyll Metabolism (ES = 0.4802, $p = 0.0459$), Adipocytokine Signaling Pathways (ES = 0.4716, $p = 0.0020$), and Butanoate Metabolism (ES = 0.5019, $p = 0.0338$). Conversely, some pathways are enriched in cluster C2: Acute Myeloid Leukemia (ES=-0.4272, $p = 0.0337$).

Discussion

AD is a progressive neurodegenerative disorder predominantly affecting the elderly population [22]. Extensive research has demonstrated that the neuropathological onset of AD precedes the manifestation of clinical symptoms over several decades [23]. As a result, it is essential to pinpoint potential biomarkers to detect AD at an early stage and to identify promising treatment strategies for its control. The dysregulation of interleukins and their receptors in AD has been a topic of interest in the field of neuroimmunology [24]. Our study confirmed the

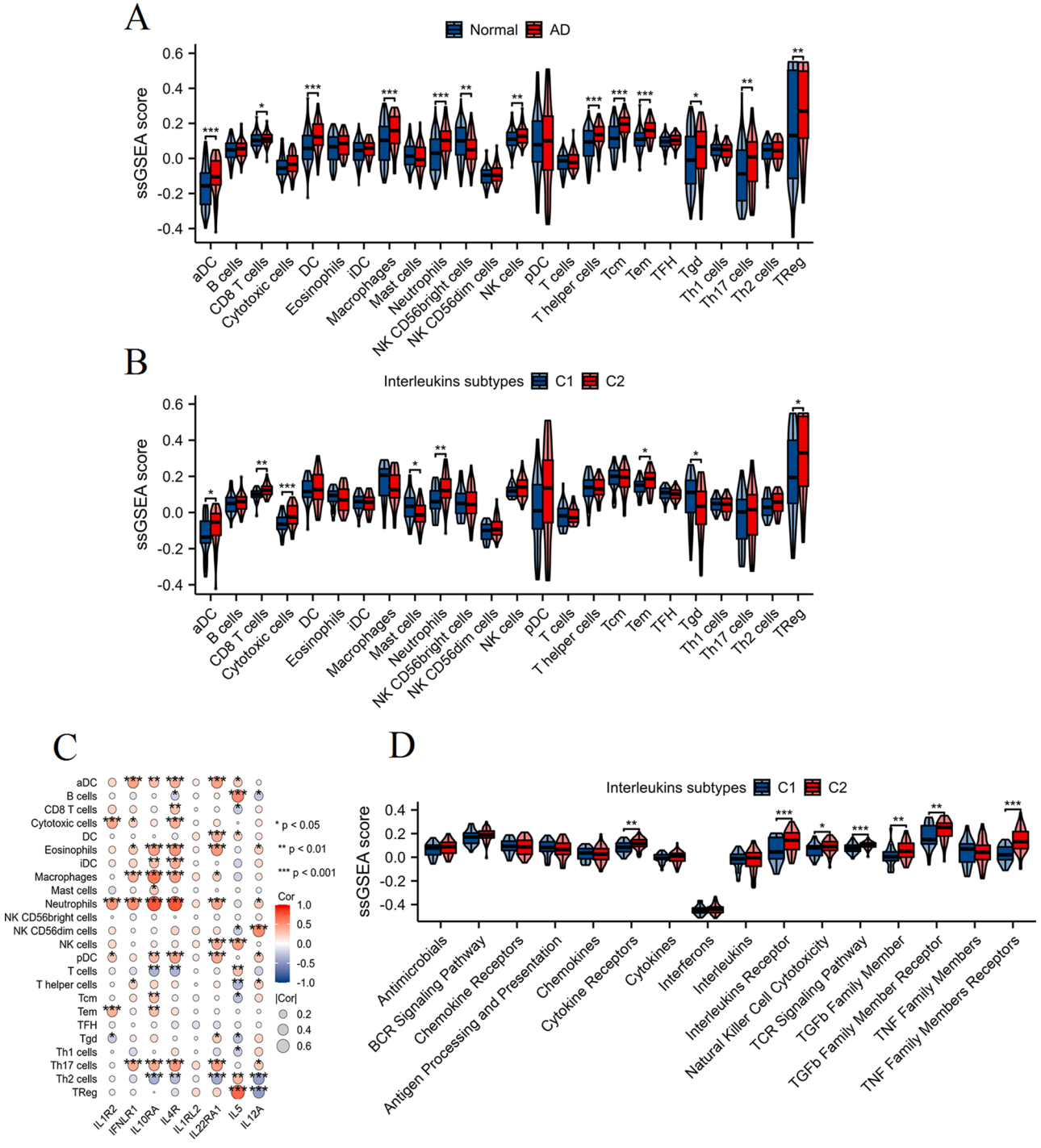

Fig. 6 Immune cell infiltration and immune-related pathway activity in AD subgroups. (**A**) Violin plots displaying ssGSEA scores for various immune cell types. (**B**) Violin plots comparing ssGSEA scores for immune cell types between AD subgroups (C1 and C2). (**C**) Heatmap showing the correlation coefficients (|Cor|) between interleukin genes and immune cell types. (**D**) Violin plots of ssGSEA scores comparing the activity of immune-related pathways. *$p < 0.05$, **$p < 0.01$, ***$p < 0.001$

upregulation of interleukins and their receptors in AD patients, which is consistent with previous reports highlighting the role of interleukin signaling in AD pathogenesis [25–27]. The identification of DIGs further supports the notion that immune dysregulation plays a crucial role in AD development and progression [28].

Our enrichment analysis revealed that the DIGs are involved in immune signaling pathways, emphasizing the importance of the immune system in AD

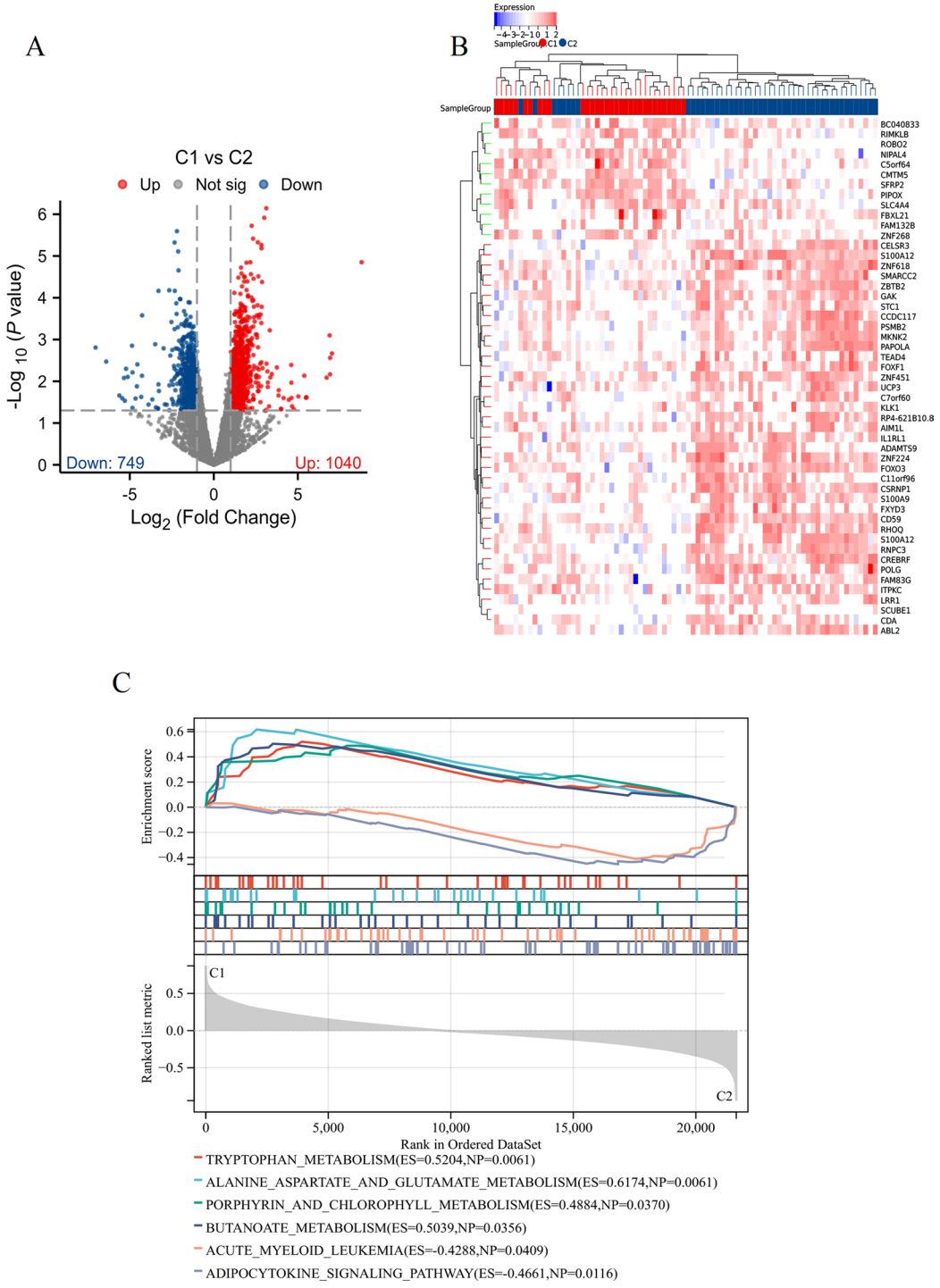

Fig. 7 Differential expression and GSEA of interleukin-related AD subgroups. (**A**) The volcano plot illustrates the differentially expressed genes (DEGs) between the two AD subgroups (C1 and C2). (**B**) Heatmap of top 50 DEGs. (**C**) GSEA plots show the top enriched pathways in cluster C1 (above) and cluster C2 (below)

pathophysiology. This finding aligns with previous studies showing the involvement of inflammatory processes and immune responses in AD pathogenesis [2930]. Furthermore, the connection between immune signaling pathways and AD pathophysiology suggests potential therapeutic targets for modulating the immune response to mitigate disease progression [31, 32]. This highlights the promising role of immunomodulation in AD treatment strategies, paving the way for novel interventions beyond traditional approaches. The predictive

nomogram based on key interleukin genes provides a novel approach to stratifying AD patients based on their interleukin gene expression levels. This personalized predictive model could potentially aid in clinical decision-making and treatment planning for AD patients.

The identification of distinct AD subgroups with different immune profiles and pathway activities adds a new dimension to our understanding of AD heterogeneity. Previous studies have shown that AD is a complex and multifactorial disease with diverse clinical presentations and underlying pathologies [33]. Our study extends these findings by highlighting the role of immune-related factors in shaping the clinical manifestations and progression of AD. By elucidating the immunological landscape of AD and identifying specific immune signatures associated with different subgroups, we pave the way for personalized classification and management strategies for AD patients. Immunological dysregulation has been increasingly recognized as a key player in the pathogenesis of AD, contributing to neuroinflammation, synaptic dysfunction, and neurodegeneration [34]. The presence of distinct immune profiles in different AD subgroups suggests that immune-mediated mechanisms may underlie the heterogeneity observed in clinical phenotypes and disease progression. For instance, specific cytokine profiles or activation of immune cell subsets may drive different pathogenic processes leading to varying degrees of cognitive decline and neurodegeneration in AD patients [35–37]. Furthermore, considering immune-related factors in the classification and management of AD patients may have important therapeutic implications. Targeting specific immune pathways or modulating immune responses based on individual immune profiles could lead to more effective and personalized treatment strategies for AD. For example, immunomodulatory therapies that target interleukin signaling or immune cell activation may be more beneficial for AD patients with certain immune profiles, while other subgroups may benefit from different treatment approaches [38, 39].

However, our study still suffers from the following limitations: The cross-sectional nature of transcriptomic data prevents definitive conclusions about whether the identified subgroups represent distinct disease entities or different temporal stages of immune activation. Longitudinal studies tracking subgroup transitions could clarify this crucial distinction. While our deconvolution algorithms estimate immune infiltration, we lack direct histological validation through immunohistochemistry or single-cell spatial analysis of brain tissues to confirm microglial activation patterns. The predictive model's clinical utility requires prospective validation in ethnically diverse populations with standardized cognitive assessments before implementation in precision medicine frameworks.

Conclusion

Overall, our study contributes to the growing body of evidence supporting the role of interleukins and immune dysregulation in AD. By providing insights into the immunological landscape of AD and identifying potential biomarkers for personalized therapeutic strategies, our findings have important implications for the development of targeted interventions for AD patients.

Supplementary Information

The online version contains supplementary material available at https://doi.org/10.1186/s12883-025-04155-y.

Supplementary Material 1

Acknowledgements
Not applicable.

Author contributions
The manuscript was authored by Bin Zhang, who also devised the study's design. Meanwhile, data analysis and figure generation were carried out by Binglei Xu, Ruoxian Zhang, and Baoying Gong. Lastly, the manuscript underwent review and editing by Jianwen Guo. All authors reviewed the manuscript.

Funding
Not applicable.

Data availability
The data utilized in our research can be accessed through the GEO database (https://www.ncbi.nlm.nih.gov/geo/).

Declarations

Ethics approval and consent to participate.
Not applicable.

Consent for publication
Not applicable.

Competing interests
The authors declare no competing interests.

Received: 29 October 2024 / Accepted: 24 March 2025
Published online: 10 April 2025

References

1. Scheltens P, De Strooper B, Kivipelto M, Holstege H, Chételat G, Teunissen CE, Cummings J, van der Flier WM. Lancet (London England). 2021;397:1577–90. Alzheimer's disease.
2. Soria Lopez JA, González HM, Léger GC. Alzheimer's disease. Handb Clin Neurol. 2019;167:231–55.
3. Byun MS, Kim SE, Park J, Yi D, Choe YM, Sohn BK, Choi HJ, Baek H, Han JY, Woo JI, Lee DY. Heterogeneity of regional brain atrophy patterns associated with distinct progression rates in Alzheimer's disease. PLoS ONE. 2015;10:e0142756.
4. Lehmann S, Dumurgier J, Schraen S, Wallon D, Blanc F, Magnin E, Bombois S, Bousiges O, Campion D, Cretin B, Delaby C, Hannequin D, Jung B, Hugon J, Laplanche JL, Miguet-Alfonsi C, Peoc'h K, Philippi N, Quillard-Muraine M, Sablonnière B, Touchon J, Vercruysse O, Paquet C, Pasquier F, Gabelle A. A diagnostic scale for Alzheimer's disease based on cerebrospinal fluid biomarker profiles. Alzheimers Res Ther. 2014;6:38.
5. Boström G, Freyhult E, Virhammar J, Alcolea D, Tumani H, Otto M, Brundin RM, Kilander L, Löwenmark M, Giedraitis V, Lleó A, von Arnim CAF, Kultima K,

Ingelsson M. Different inflammatory signatures in Alzheimer's disease and frontotemporal dementia cerebrospinal fluid. J Alzheimer's Disease: JAD. 2021;81:629–40.
6. Chai YL, Lee JH, Chong JR, Ballard C, Francis PT, Kennedy BK, Arumugam TV, Chen CP, Aarsland D, Lai MKP. Inflammatory panel cytokines are elevated in the neocortex of late-stage Alzheimer's disease but not lewy body dementias. J Neuroinflamm. 2023;20:111.
7. Pan H, Wang G, Bi Z, Lai C, Wang M. Identification of key neutrophil extracellular trap genes in Alzheimer's disease. J Alzheimer's Disease: JAD. 2024;102:1027–41.
8. Rostagno AA. Pathogenesis of Alzheimer's Disease. Int J Mol Sci 24 (2022).
9. Ogbodo JO, Agbo CP, Njoku UO, Ogugofor MO, Egba SI, Ihim SA, Echezona AC, Brendan KC, Upaganlawar AB, Upasani CD. Alzheimer's Disease: Pathogenesis and Therapeutic Interventions. Current aging science 15 (2022) 2–25.
10. Thakur S, Dhapola R, Sarma P, Medhi B, Reddy DH. Neuroinflammation in Alzheimer's disease: current progress in molecular signaling and therapeutics. Inflammation. 2023;46:1–17.
11. Leng F, Edison P. Neuroinflammation and microglial activation in alzheimer disease: where do we go from here? Nature reviews. Neurology. 2021;17:157–72.
12. Sarkar S, Biswas SC. Astrocyte subtype-specific approach to Alzheimer's disease treatment. Neurochem Int. 2021;145:104956.
13. Younas A, Younas N, Iqbal MJ, Ferrer I, Zerr I. Comparative interactome mapping of Tau-protein in classical and rapidly progressive Alzheimer's disease identifies subtype-specific pathways. Neuropathol Appl Neurobiol. 2024;50:e12964.
14. Lyra ESNM, Gonçalves RA, Pascoal TA, Lima-Filho RAS, Resende EPF, Vieira ELM, Teixeira AL, de Souza LC, Peny JA, Fortuna JTS, Furigo IC, Hashiguchi D, Miya-Coreixas VS, Clarke JR, Abisambra JF, Longo BM, Donato J Jr., Fraser PE, Rosa-Neto P, Caramelli P, Ferreira ST. De Felice, Pro-inflammatory interleukin-6 signaling links cognitive impairments and peripheral metabolic alterations in Alzheimer's disease. Translational Psychiatry. 2021;11:251.
15. Babić Leko M, Nikolac Perković M, Klepac N, Štrac D, Borovečki F, Pivac N, Hof PR, Šimić G. IL-6, IL-10, and TNFα single nucleotide polymorphisms in human influence the susceptibility to Alzheimer's disease pathology. J Alzheimer's Disease: JAD. 2020;75:1029–47.
16. Fu AK, Hung KW, Yuen MY, Zhou X, Mak DS, Chan IC, Cheung TH, Zhang B, Fu WY, Liew FY, Ip NY. IL-33 ameliorates Alzheimer's disease-like pathology and cognitive decline. Proc Natl Acad Sci USA. 2016;113:E2705–13.
17. Quintanilla RA, Orellana DI, González-Billault C, Maccioni RB. Interleukin-6 induces Alzheimer-type phosphorylation of Tau protein by deregulating the cdk5/p35 pathway. Exp Cell Res. 2004;295:245–57.
18. Yang R, Duan J, Luo F, Tao P, Hu C. IL-6, IL-8 and IL-10 polymorphisms May impact predisposition of Alzheimer's disease: a meta-analysis. Acta Neurol Belgica. 2021;121:1505–12.
19. Di Bona D, Plaia A, Vasto S, Cavallone L, Lescai F, Franceschi C, Licastro F, Colonna-Romano G, Lio D, Candore G, Caruso C. Association between the interleukin-1beta polymorphisms and Alzheimer's disease: a systematic review and meta-analysis. Brain Res Rev. 2008;59:155–63.
20. Mun MJ, Kim JH, Choi JY, Jang WC. Genetic polymorphisms of Interleukin genes and the risk of Alzheimer's disease: an update meta-analysis. Meta Gene. 2016;8:1–10.
21. Yang X, Su X, Wang Z, Yu Y, Wu Z, Zhang D. ULBP2 is a biomarker related to prognosis and immunity in colon cancer. Mol Cell Biochem. 2023;478:2207–19.
22. Dong X, Nao J, Shi J, Zheng D. Predictive value of routine peripheral blood biomarkers in Alzheimer's disease. Front Aging Neurosci. 2019;11:332.
23. Vermunt L, Sikkes SAM, van den Hout A, Handels R, Bos I, van der Flier WM, Kern S, Ousset PJ, Maruff P, Skoog I, Verhey FRJ, Freund-Levi Y, Tsolaki M, Wallin K, Olde Rikkert ÅM, Soininen H, Spiru L, Zetterberg H, Blennow K, Scheltens P, Muniz-Terrera G, Visser PJ. Duration of preclinical, prodromal, and dementia stages of Alzheimer's disease in relation to age, sex, and APOE genotype. Alzheimer's Dement J Alzheimer's Assoc. 2019;15:888–98.
24. Weisman D, Hakimian E, Ho GJ. Interleukins, inflammation, and mechanisms of Alzheimer's disease. Vitam Horm. 2006;74:505–30.
25. Calsolaro V, Edison P. Neuroinflammation in Alzheimer's disease: current evidence and future directions. Alzheimer's Dement J Alzheimer's Assoc. 2016;12:719–32.
26. Zheng C, Zhou XW, Wang JZ. The dual roles of cytokines in Alzheimer's disease: update on interleukins, TNF-α, TGF-β and IFN-γ. Translational Neurodegeneration. 2016;5:7.
27. Mohammadi Shahrokhi V, Ravari A, Mirzaei T, Zare-Bidaki M, Asadikaram G, Arababadi MK. IL-17A and IL-23: plausible risk factors to induce age-associated inflammation in Alzheimer's disease. Immunol Investig. 2018;47:812–22.
28. Guo Z, Peng X, Li HY, Wang Y, Qian Y, Wang Z, Ye D, Ji X, Wang Z, Wang Y, Chen D, Lei H. Evaluation of peripheral immune dysregulation in Alzheimer's disease and vascular dementia. J Alzheimer's Disease: JAD. 2019;71:1175–86.
29. McGeer PL, McGeer EG. The amyloid cascade-inflammatory hypothesis of alzheimer disease: implications for therapy. Acta Neuropathol. 2013;126:479–97.
30. Sudduth TL, Schmitt FA, Nelson PT, Wilcock DM. Neuroinflammatory phenotype in early Alzheimer's disease. Neurobiol Aging. 2013;34:1051–9.
31. Jorfi M, Maaser-Hecker A, Tanzi RE. The neuroimmune axis of Alzheimer's disease. Genome Med. 2023;15:6.
32. Uddin MS, Kabir MT, Jalouli M, Rahman MA, Jeandet P, Behl T, Alexiou A, Albadrani GM, Abdel-Daim MM, Perveen A, Ashraf GM. Neuroinflammatory signaling in the pathogenesis of Alzheimer's disease. Curr Neuropharmacol. 2022;20:126–46.
33. Alkadhi K, Eriksen J. The complex and multifactorial nature of Alzheimer's disease. Curr Neuropharmacol. 2011;9:586.
34. Liu YH, Zeng F, Wang YR, Zhou HD, Giunta B, Tan J, Wang YJ. Immunity and Alzheimer's disease: immunological perspectives on the development of novel therapies. Drug Discovery Today. 2013;18:1212–20.
35. Keren-Shaul H, Spinrad A, Weiner A, Matcovitch-Natan O, Dvir-Szternfeld R, Ulland TK, David E, Baruch K, Lara-Astaiso D, Toth B, Itzkovitz S, Colonna M, Schwartz M, Amit I. A unique microglia type associated with restricting development of Alzheimer's disease. Cell. 2017;169:1276–e129017.
36. Gate D, Saligrama N, Leventhal O, Yang AC, Unger MS, Middeldorp J, Chen K, Lehallier B, Channappa D, De Los Santos MB, McBride A, Pluvinage J, Elahi F, Tam GK, Kim Y, Greicius M, Wagner AD, Aigner L, Galasko DR, Davis MM. Wyss-Coray, clonally expanded CD8 T cells patrol the cerebrospinal fluid in Alzheimer's disease. Nature. 2020;577:399–404.
37. Hickman SE, Khoury JE. Mechanisms of mononuclear phagocyte recruitment in Alzheimer's disease. CNS Neurol Disord Drug Target. 2010;9:168–73.
38. Latta CH, Brothers HM, Wilcock DM. Neuroinflammation in Alzheimer's disease; A source of heterogeneity and target for personalized therapy. Neuroscience. 2015;302:103–11.
39. Wang H, Shen Y, Chuang H, Chiu C, Ye Y, Zhao L. Neuroinflammation in Alzheimer's disease: microglia, molecular participants and therapeutic choices. Curr Alzheimer Res. 2019;16:659–74.

Publisher's note